Influence of bottoming-bead geometry in wipe bending process

Supak Chanthapak*, Chulsiri Sringamphong and Sutasn Thipprakmas

Department of Tool and Materails Engineering,
King Mongkut's University Technology Thonburi, Bangkok, Thailand 10400
* Corresponding Author: E-mail: 52404209@st.kmutt.ac.th

Abstract

Wipe bending process is widely used in the hard disk drive industry. The major problem in this process is a springback. The springback can be reduced by using a bottoming technique. In this paper, the influences of bottoming-bead geometry on springback were investigated by using finite element method (FEM) and the FEM simulation results were validated by laboratory experiments. Workpiece material used in this research is a low-carbon steel, SPCC (JIS G 3141). The commercial code, DEFORM-2D, was used. The mechanism of springback when the bottoming technique applied was clearly identified based on the stress distribution. The influences of bottoming-bead geometry on springback were also clearly identified. The FEM simulation results showed a good agreement with the experimental results.

Keywords*:* Wipe Bending / Bottoming / FEM / Springback

1. Introduction

Wipe bending is one of common applications to deform the L-shaped part in sheet metal forming procedure. After bending operation, the angle of workpiece becomes greater than the die angle, which referred to the springback. The occurrence of springback is the major problem in bending process that caused dimension error of bended part.

The previous research has been done on the springback prediction by using finite element analysis (FEA). Livatyali et al [1, 2] had evaluated the amount of springback in straight flanging by using FEM to predict and reduce the springback. The first part is the experimental investigations on the effect of process variables on springback. The second part covers the FEA of flanging and found that the result from FEA had good agreement with the experimental results. Ling et al [3] studied L-bending die design by using finite element methods. The results provide the better understanding of die parameters, including die clearance, die radius, step height and step distance which affect the springback. Chen and Ko [4] examined the phenomenon in mechanics of the springback deformation in the L-bending of sheet-metal and reduced springback by a Reverse Bend Approach. Thipprakmas and Rojananan [5] investigated the spring-go phenomenon by using the FEM on the V-bending process. Panthi et al [6] observed the influence of geometric parameters, material properties (yield

stress, Young's modulus, strain hardening), and lubrication condition on the springback by using RRL-FEM software. The results showed that the springback highly depends on material properties and geometric parameters whereas friction has negligible effect on the springback.

In this study, the influence of bottoming bead geometry, including bead width, bead height and die radius on springback were investigated by using FEM. The stress distribution was used to explain the mechanism of springback when the bottoming technique applied in wipe bending. The springback value from the FEM simulation results were validated by laboratory experiments.

2. Finite element simulation and experiments

2.1 Finite element simulation model.

Sheet metal wipe bending can be simplified to two-dimensional problem. Fig. 1 shows the finite element model of the wipe bending simulation that was considered based on plane strain model. The bottoming-bead geometry parameters were shown in Fig. 2. The workpiece material was low-carbon steel, SPCC (JIS G 3141) with thickness of 1.0 mm. The bead width (w) of 0.5, 1.0, 1.5 mm, the bead height (h) of 0.05, 0.10, 0.15, 0.20 mm, and die radius (R_d) of 0.1, 0.3, and 0.5 mm were investigated as shown in table 1. Die clearance was equal to the sheet thickness 1.0 mm.

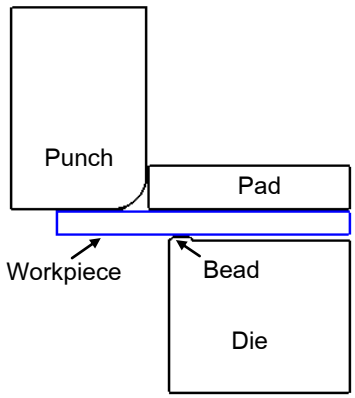

Fig. 1 Finite element simulation model

2.2. Finite element simulation conditions

In this study, the commercial software DEFORM-2D was used as FEM simulation tool. The workpiece material behavior was assumed to be elasto-plastic type while punch, die and blankholder were assumed to be rigid type. The mechanical properties of workpiece as shown in Table 1 were collected from the tensile test.

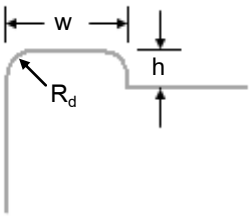

Fig. 2 Bottoming bead geometry parameter

Table. 1 Finite element simulation conditions

Simulation model	Plane strain
Object type	Workpiece : Elasto-plastic Punch/Die : Rigid Blankholder : Rigid
Material	SPCC Thickness = 1.0 mm
Flow curve	$\bar{\sigma} = 532.84\,\bar{\varepsilon}^{0.29} + 326.19$
Elastic Modulus	210 GPa
Poisson's Ratio (ν)	0.3
Friction coefficient (μ)	0.12
Bead width (w)	0.5, 1.0, 1.5 mm
Bead height (h)	0.05, 0.10, 0.15, 0.20 mm
Die radius (R_d)	0.1, 0.3, 0.5 mm
Punch radius (R_p)	1.5 mm
Die clearance (Cl)	1.0 mm

In finite element simulation, more elements per unit area offers increased accuracy and resolution of geometry. However, in general, the time required for the computer to solve the problem increases as number of nodes increases. Considering the effect of the number of elements, difference cases were evaluated to find out a suitable number of elements. A plotted graph of the bending angle and number of elements is shown in Fig. 3. At the elements greater than 2,000 were found to be converged. Thus approximately 2,000 elements were applied for all of simulations. The finer mesh was generated between punch and die in order to obtain more accurate results.

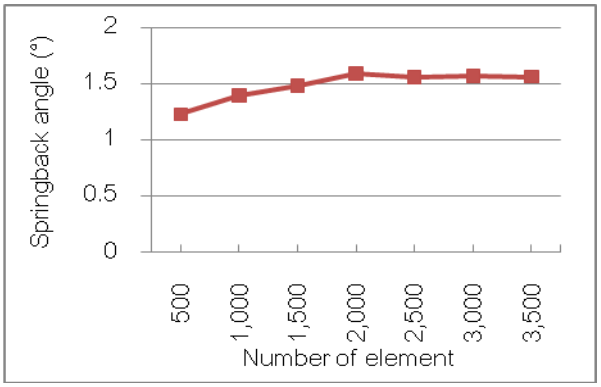

Fig. 3 Effect of number of element to springback angle

2.2. Experimental procedure

The experiments were carried out to validate the accuracy of FEM simulation results. The specimens were bent to 90° by the wipe bending die set as shown in Fig. 4. In this study, the wipe bending die set was placed on the universal tensile testing machine as shown in Fig. 5. After bending operations, the bending angle was measured by measuring microscope with Motic Images program. Then, the springback angle from the experiments will be compared with the simulations results.

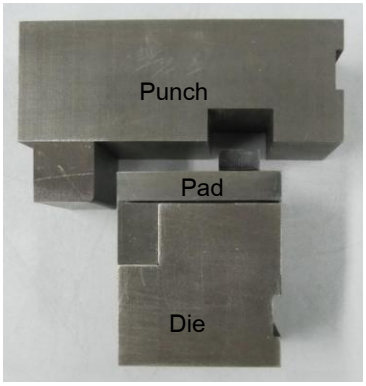

Fig. 4 Wipe bending die

Fig. 5 Wipe bending die set on universal tensile testing machine

3. Results and Discussion

3.1 Stress distribution analysis

Before analyze the effect of bottoming-bead geometry, observe the stress distribution in the conventional wipe bending. Fig. 6 shows the mean stress distribution at the end of bending stroke in bend part which obtained from the simulation of conventional wipe bending with punch radius 1.5 mm and die radius 1.0 mm. Over the die radius, the maximum tensile stress appeared at the outer surface and decreased inward into the material thickness. On the other hand, the maximum compressive stress appeared

at the inner surface and also decreased inward into the material thickness. The elastic recovery was generated in the area on the neutral axis,

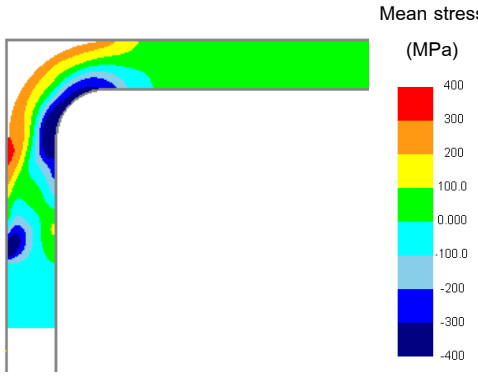

Fig. 6 Stress distribution in bend part

which is called the elastic band, caused the springback to occur after the punch was removed.

3.1.1 Influence of bead width

Fig. 7 shows the mean stress distribution at the end of bending stroke in the bend part with respect to the bead width of 0.5, 1.0, and 1.5 mm, bead height of 0.1 mm, and die radius of 0.1, 0.3, and 0.5 mm. The occurrence of compressive stress at the bottoming area could eliminate the elastic recovery at the corner of the bend part. As the results showed the more bead width was, the more compressive stress was generated. Furthermore, at the bent leg in the cases of bead width of 1.0 and 1.5 mm, the compressive stress was generated at the outer surface while the tensile stress appeared at the inner surface and decreased inward into the material thickness. This feature caused the reversed stress distribution compared with the bending zone in case of conventional wipe bending.

3.1.2 Influence of bead height

To analyze the influence of bead height, Fig. 8 shows the mean stress distribution at the end of bending stroke in the bend part with respect to the bead height of 0.05, 0.10, 0.15,

Bead width (mm)	Die radius (mm)		
	0.1	0.3	0.5
0.50			
1.00			

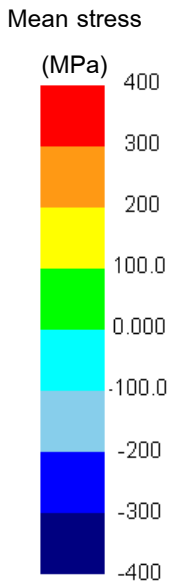

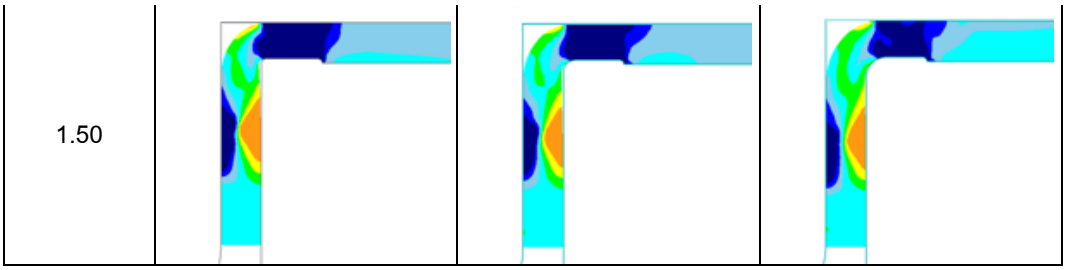

Fig. 7 Influence of bead width on mean stress distribution

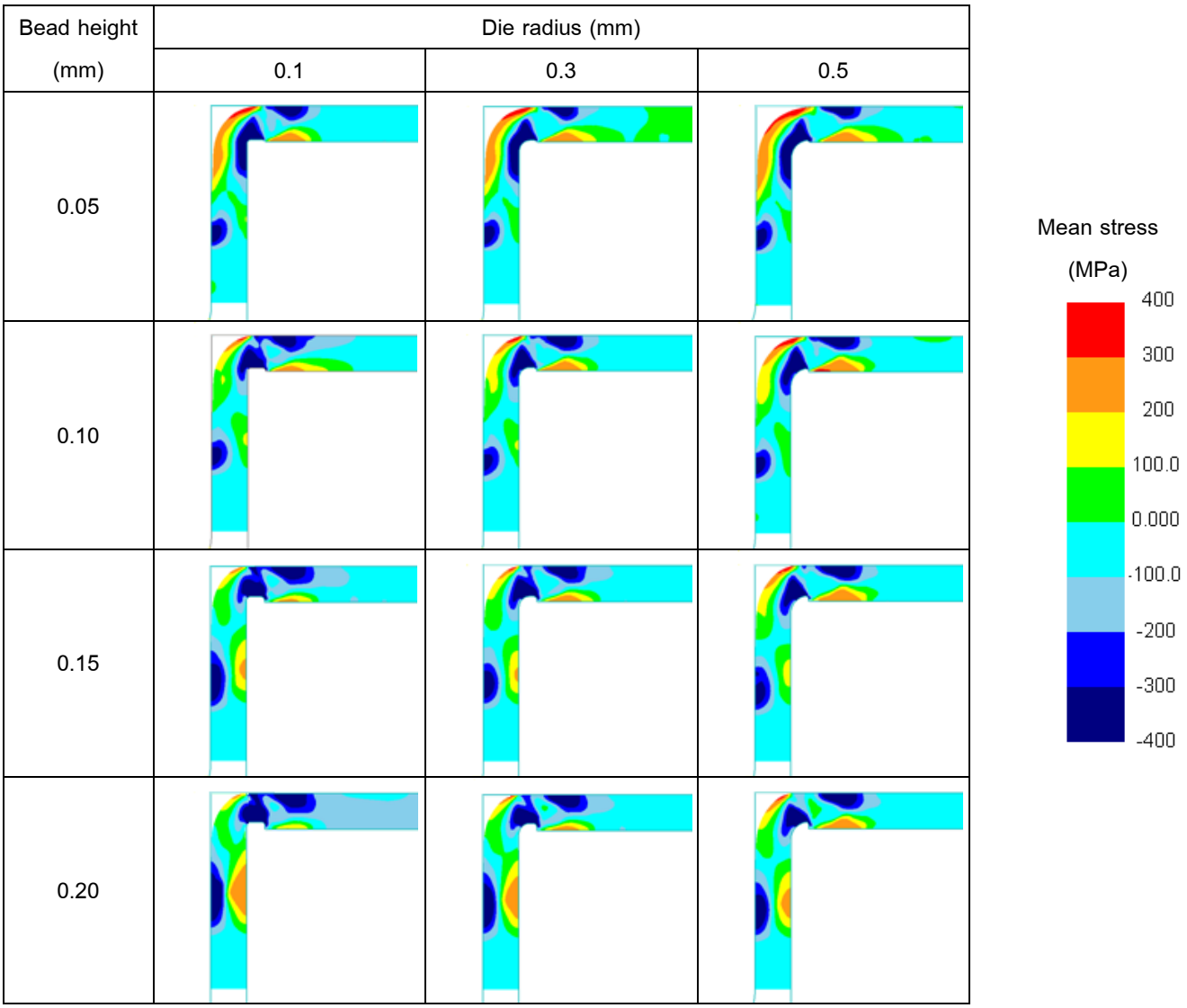

Fig. 8 Influence of bead height on mean stress distribution

and 0.20 mm and die radius of 0.1, 0.3, and 0.5 mm. Similarly, the compressive stress was generated at the bottoming area that could reduce the elastic recovery at the corner of the bend part. As the results showed the increasing of bead width cause the compressive stress increased. In case of bead height of 0.15 mm, the compressive stress was generated at the outer surface of bent leg while the tensile stress appeared at the inner surface, caused the

reversed stress distribution compared with the bending zone in case of conventional wipe bending.

3.1.3 Influence of die radius

Considering effect of die radius, the stress distribution with respect to die radius of 0.1, 0.3, and 0.5 mm was shown in Fig. 7 and 8. The decreasing of die radius caused the slightly decreasing of elastic zone at bent leg. When compared with the effect of bead width and height, the die radius has negligible effect on stress distribution.

3.2 Springback angle

3.2.1 Influence of bead width

Fig. 9 shows the plotted graph of springback angle with respect to the bead width of 0.5, 1.0, and 1.5 mm, bead height of 0.1 mm, and die radius of 0.1, 0.3, and 0.5 mm from simulations. The springback angle in every case of bead width was negative values, which is called the spring-go. The result shows that the spring-go angle increased as the bead width increased.

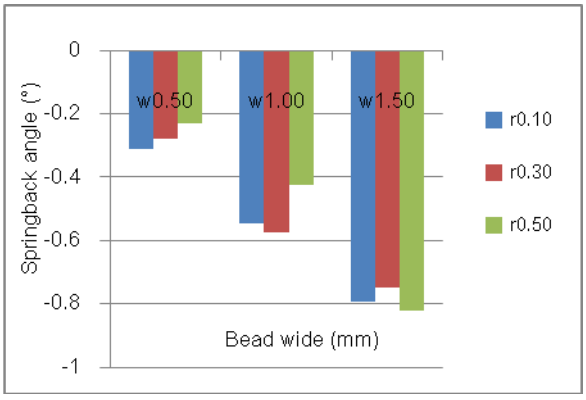

Fig. 9 Influence of bead width on springback angle from simulations

3.2.2 Influence of bead height

Fig. 10 shows the plotted graph of springback angle with respect to the bead height of 0.05, 0.10, 0.15, and 0.20 mm and die radius of 0.1, 0.3, and 0.5 mm. The spring-go phenomenon was found in case of bead height 0.10, 0.15, and 0.20 mm. and increased with the increasing of bead height.

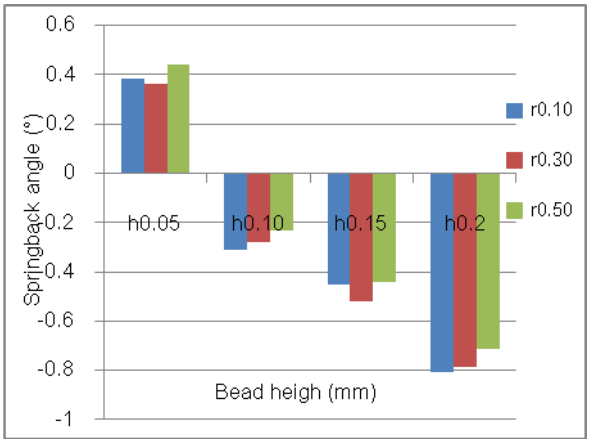

Fig. 10 Influence of bead height on springback angle from simulations

3.3 Comparing FE simulation and experimental results

To validate the accuracy of FEM simulation results the experiments were carried out. The conventional wipe bending and difference 4 cases of bottoming bead geometry (r0.1w0.5h0.1, r0.1w1.0h0.1, r0.1w0.5h0.2, and r0.1w0.5h0.1) were used to determined the influence of bead width, height, and radius.

3.3.1 Springback angle

Comparison of springback angle between the FEM simulations and the experiments was shown in Fig.11. In this study, it was observed that the springback angle obtained by the experiments were slightly higher than the simulation results.

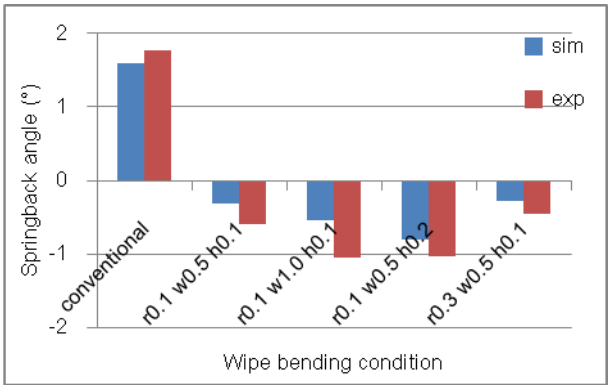

Fig. 11 Comparison of springback angle between FEM simulation and experiments

3.3.2 Bending force

Comparison of bending force between the FEM simulations and the experiments in case of die radius of 0.1 mm, bead width of 0.5 mm, and bead height of 0.1 mm was also observed as shown in Fig. 12. The FEM simulations results confirmed good agreement with the experimental results.

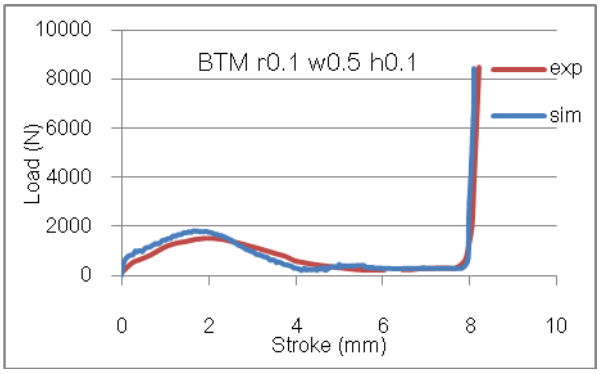

Fig. 12 Bending force between FE simulation and experimental

4. Conclusions

In this study, Influence of of bottoming bead geometry on springback in the wipe bending of sheet metal was investigated by using FEM and experiments. From the results, it can be concluded as follows;

1. The springback values could be reduced by bottoming technique while the excessive bead geometry caused the negative values of springback angle, called the spring-go.

2. The increasing of bead geometry generated more compressive stress at the bottoming area that could eliminate the elastic recovery at the corner of the bend part resulted in the decrease in the springback.

3. The increasing of bead geometry also caused the reversed stress distribution at bent leg compared with the bending zone resulted in the increase in the spring-go.

5. Acknowledgement

Special thanks to the Advanced Manufacturing Industry/University Cooraperative Research Center, King Mongkut's University of Technology Thonburi, Thailand for their financial assistance to this study.

6. References

[1] H. Livatyalia and T. Altanb. (2001). Prediction and elimination of springback in straight flanging using computer-aided design methods Part 1.Experimental investigation, *Journal of Materials Processing Technology,* Vol. 117, pp. 262–268.

[2] H. Livatyalia, H.C. Wub, T. Altanb. (2002). Prediction and elimination of springback in straight flanging using computer-aided design methods Part 2: FEM predictions and tool design, *Journal of Materials Processing Technology,* Vol. 120, pp. 348–354.

[3] Ling YE, Lee HP, Cheok BT. (2005). Finite element analysis of springback in L-bending of sheet metal, *Journal of Materials*

Processing Technology, Vol. 168, pp. 296–302.

[4] F.K. Chen and S.F. Ko. (2006). Deformation analysis of spring-back in L-bending of sheet metal, *Journal of Achievements in Materials and Manufacturing Engineering,* Vol. 18, pp. 339-342.

[5] Thipprakmas S, Rojananan S. (2008). Investigation of spring-go phenomenon using finite element method, *Materials and Design,* Vol. 29, pp. 1526–1532.

[6] S.K. Panthi, N. Ramakrishnan, M. Ahmed, S.S. Singh and M.D. Goel. (2010). Finite element analysis of sheet metal bending process to predict the springback, *Materials and Design,* Vol. 31, pp. 657-662.